Appl. Phys. B 57, 167–176 (1993)

Applied Physics B Photophysics and Laser Chemistry

Suppression of Stimulated Hyper-Raman Scattering in Lithium Vapor

Mao-hong LU, Yu-mei LIU

Institute of Electro-optical Engineering, National Chiao-Tung University, Hsinchu, Taiwan 30050, ROC
(Fax: +886-35/716631)

Received 20 January 1993/Accepted 15 June 1993

Abstract. The stimulated hyper-Raman scattering (SHRS) in lithium vapor has been observed in both the forward and the backward directions as the laser was tuned near the 2S–3S and 2S–4S two-photon resonances. It is found that in the forward direction the SHRS associated with the 2P excitation near the 2S–3S or the 2S–4S two-photon resonance is completely suppressed, but the SHRS associated with the 3P excitation near the 2S–4S two-photon resonance can be observed. A condition under which the forward SHRS takes place, given by Malakyan [3], has been examined. A reasonable agreement between the theory and the experiment is obtained. Near the 2S–3S two-photon resonance, instead of the expected emission ω_{2P-2S} corresponding to the 2P–2S transition, an emission at the $2\omega_P - \omega_{3S-2P}$ frequency, which is close to the ω_{2P-2S}, has been observed in the backward direction. The process generating this emission could be considered as an inverse SHRS process induced by the 3S–2P spontaneous emission. For the SHRS emission a shift of the observed frequency from the calculated frequency has been found. In order to explain the shift, the Stark effect has been calculated. The results show that the shift can not be attributed to the Stark effect.

PACS: 32.00, 42.65.Dr

A suppression of stimulated hyper-Raman scattering (SHRS) near the 3S–3D or 3S–4D two-photon resonance of sodium was observed and discussed first by Moore et al. [1] and then by Wunderlich et al. [2]. They explained this suppression process as a destructive interference between two excitation pathways connecting the ground and the excited states, as shown in Fig. 1. One of the pathways is the SHRS process involving the absorption of two laser photons and the stimulated emission of a SHRS photon. The other pathway is created by a new field generated by a four-wave mixing process (FWM), in which two laser photons are coupled with the SHRS photon. If the phase-matching is considered for the FWM process, the SHRS suppression would occur only in the forward direction. In other words, the SHRS in the backward direction is not influenced. The suppression process of SHRS was also analyzed theoretically by Malakyan [3], who called this suppression process a self-induced suppression because the pathway which suppresses the SHRS is induced by the SHRS itself in the FWM process. According to her analysis, the forward SHRS will take place if the following condition is met,

$$R = \omega_2 \mu_{23}^2 \Omega^2 / \omega_3 \mu_{31}^2 \Delta^2 \approx f_{32} \Omega^2 / f_{13} \Delta^2 > 1 \,, \tag{1}$$

where ω_2 and ω_3 are the frequencies of SHRS and the new field produced by FWM, respectively, μ_{ij} and f_{ij} are the dipole matrix element and the oscillator strength of the $i \to j$ transition, respectively, $\Delta = 2\omega_P - \omega_{21}$ denotes the detuning from the two-photon resonance ω_{21} (see Fig. 1) and Ω is the two-photon Rabi frequency defined by

$$\Omega = \left| \sum_m \frac{\mu_{2m}\mu_{m1}}{(2\hbar)^2(\omega_{m1} - \omega_P)} A_P^2 \right| \quad \text{(rad/s)}$$

or

$$\Omega = \frac{1}{2nc\varepsilon_0\hbar^2} \left| \sum_m \frac{\mu_{2m}\mu_{m1}}{(\omega_{m1} - \omega_P)} \right| I_P \quad \text{(rad/sec)} \,. \tag{2}$$

Here A_P is the amplitude of the laser field:

$$\mathbf{E}_P = \frac{1}{2} \hat{\mathbf{e}}_P A_P e^{-i\omega_P t + ik_P z} + \text{c.c} \tag{3}$$

and $I_P = \frac{1}{2} n \varepsilon_0 |A_P|^2$ is the laser intensity, $h = 2\pi\hbar$ is the Planck constant, ω_{ij} is the transition frequency from the i state to the j state, $\hat{\mathbf{e}}_P$ is the unit vector along the laser polarization, n is the refractive index, and ε_0 and c are the permittivity and the light velocity in free space, respectively.

In this paper we present some results from the observation of SHRS in lithium vapor as the laser wavelength is tuned near the 2S–3S and the 2S–4S two-photon resonances. Our primary intent is to examine the condition (1). The energy-level diagram of lithium is shown in Fig. 2 [4], where the SHRS processes expected to be observed are also illustrated. In sodium the results of [1, 2] show

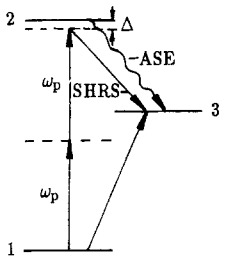

Fig. 1. Energy-level diagram showing a destructive interference between two pathways connecting the states 1 and 3

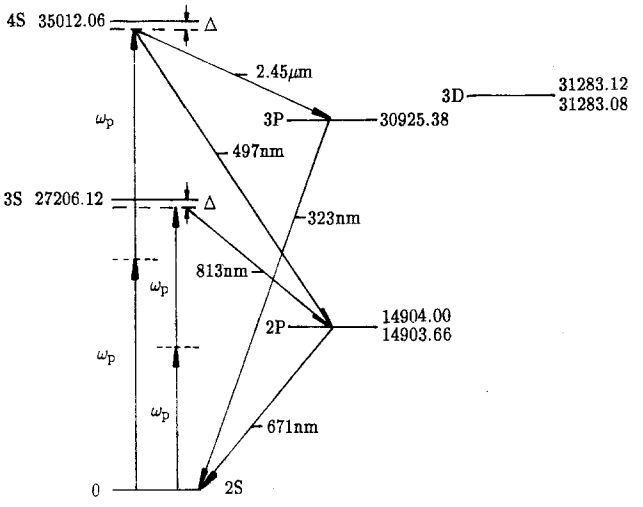

Fig. 2. Energy-level diagram of lithium. The SHRS processes expected to be observed are illustrated

that near the 3S–4D two-photon resonance there exists an axially phase-matched parametric four-wave mixing (PFWM) in which the wavelength of a generated field is in close proximity to that of SHRS associated with the 4P excitation. Since both the axial PFWM emission and the SHRS emission overlap in space and have a similar feature for laser tuning, it is difficult to distinguish one from the other. However, in lithium on or near the 2S–3S and 2S–4S two-photon resonances a calculation, as we did in [5], shows that there exists not any axially phase-matched PFWM in which the wavelength of the generated field is near that of the SHRS associated with the 2P or 3P excitation. Compared with the frequency uncertainty of two-photon pumping $\sim 0.5\ \mathrm{cm}^{-1}$ in this experiment due to the laser linewidth $\sim 0.25\ \mathrm{cm}^{-1}$, the splitting of fine structure of lithium, that is $\sim 0.3\ \mathrm{cm}^{-1}$ for the 2P state and $< 0.01\ \mathrm{cm}^{-1}$ for the 3P state, will be ignored.

The Stark effect caused by the pump field is calculated under our experimental conditions in order to explain the shifts of some spectral lines observed in this experiment. Two types of contributions to the Stark shift are included. One is due to the normal optical Stark effect, given by

$$\delta_i^{(1)} = -\frac{I_P}{2n\varepsilon_0 c\hbar^2} \sum_m |\mu_{im}|^2 \left(\frac{1}{\omega_{mi} - \omega_P} + \frac{1}{\omega_{mi} + \omega_P} \right), \quad i = 1, 2, 3 . \tag{4}$$

The other is due to the two-photon Rabi frequency, given by [3]

$$\delta_i^{(2)} = -\frac{\Omega^2}{\Delta}, \qquad i = 1, 2 . \tag{5}$$

In this paper we also calculate the condition (1) for the SHRS associated with the 4P excitation of sodium near the 3S–4D two-photon resonance under the experimental condition of [2].

1 Experiment

The experimental setup is schematically shown in Fig. 3. A pulsed dye laser (Quanta-Ray, PDL-1) pumped by a Nd^{3+} : YAG laser was used as the light source. The operating parameters of the dye laser were: 20 ns pulse duration, 2–8 mJ energy per pulse, 0.25 cm^{-1} linewidth, and 10 Hz repetition rate. The dyes LDS751 and R590 (Exciton) were used for the 2S–3S and 2S–4S two-photon excitation, respectively. In this experiment linearly polarized light was used.

A conventional heat pipe was operated with lithium vapor at a temperature of 740–760°C with a 30 cm heated zone. The lithium concentration was determined by the temperature of the heat pipe at a constant buffer gas pressure of 2 mbar so that at lower vapor pressures the heat pipe was not operating in the typical heat pipe mode. Here

Fig. 3. Experimental setup

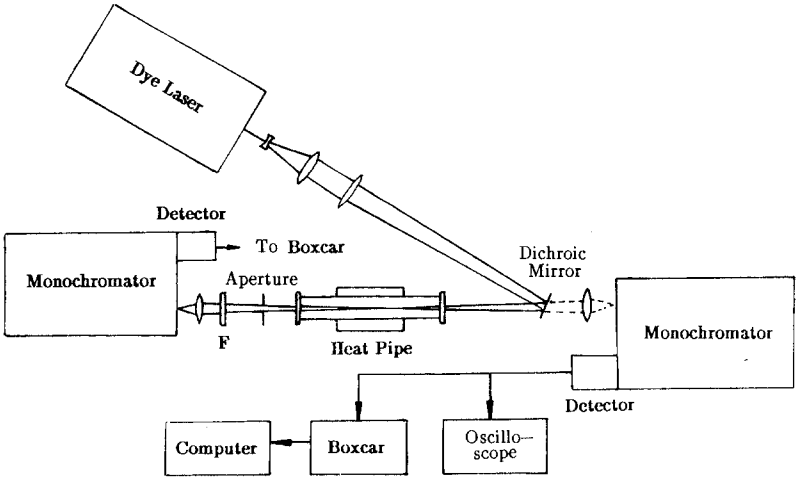

argon was used as buffer gas. The laser beam was directed along the axis of the heat pipe by a dichroic mirror, chosen to reflect the laser beam and transmit the backward emission generated from the heat pipe. The laser beam was focused by an 80 cm focal-length lens to a spot with a diameter of 0.25 mm at the center of the heat pipe. An aperture or a beam stop was placed behind the heat pipe and used to separate axial and conical parts of the generated emissions. For the forward measurement different filters were used against the strong pumping light. The output emissions were detected in both the forward and backward directions by a photomultiplier (Hamamatsu R928) in the visible region and by a Si/PbS two-color IR detector (Spex 1429C) in the infrared region after a 1 m monochromator (Spex 1704). The wavelength measurement system was calibrated by the emission lines of a CdHg lamp and a HeNe laser. The signal from the detector was fed into a boxcar averager (NF BX531) and then processed by a microcomputer.

2 Results and Discussion

As the laser wavelength was tuned on or near the 2S–3S two-photon resonance (735.13 nm), the output emissions in both forward and backward directions were measured. The results are shown in Figs. 4–6. The spectra of the emissions near the 3S–2P transition are shown in Fig. 4a, b and those near the 2P–2S transition in Fig. 5a, b. In this case three processes including amplified spontaneous emission (ASE), SHRS and FWM are involved. According to the different spectral and spatial features of the emissions generated from different processes, these emissions can be identified. From Fig. 4a, where the measurement is made in the forward direction, it can be seen that there are two different emissions. One has a fixed wavelength corresponding to the 3S–2P transition as the laser is detuned from the 2S–3S two-photon resonance, and should be considered as ASE, which results from a real transition 3S–2P accompanied with a population transfer. The other

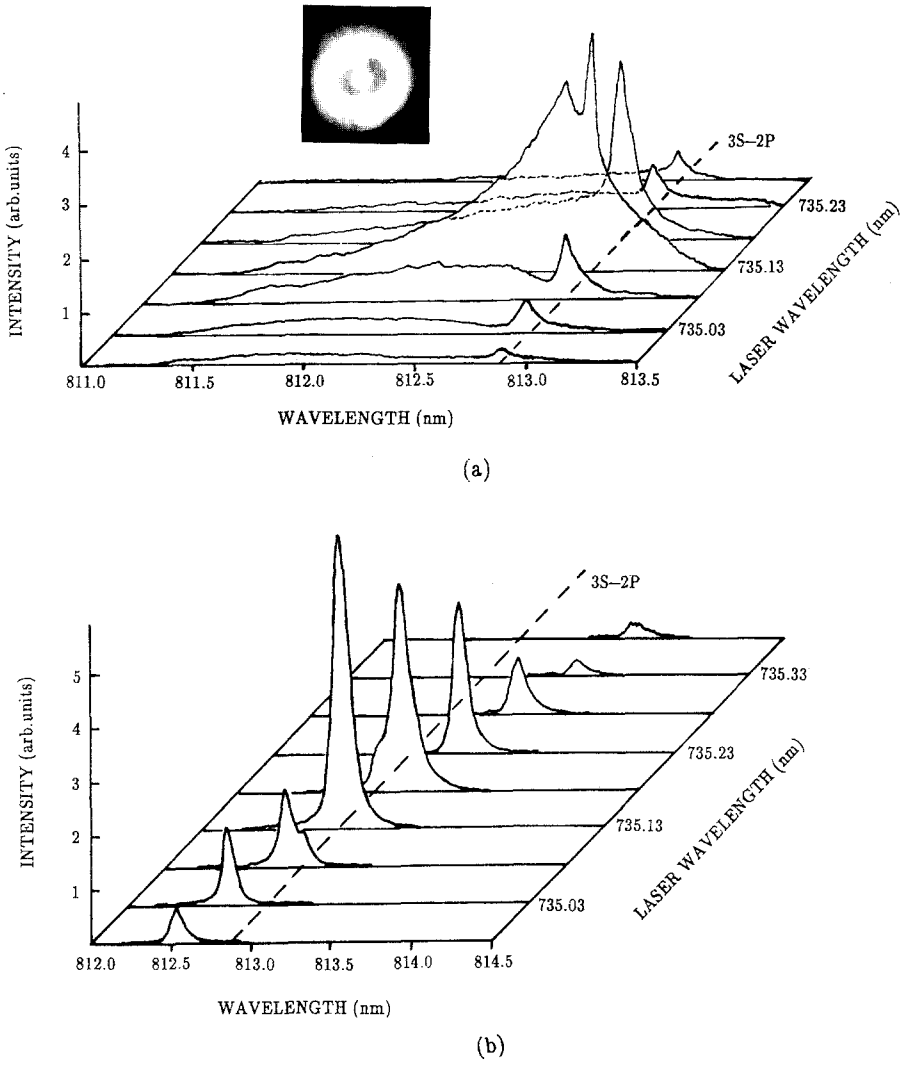

Fig. 4a, b. Spectra of the emissions near the 3S–2P transition measured in the forward direction (**a**) and in the backward direction (**b**) as the laser is tuned near the 2S–3S two-photon resonance (735.13 nm). In the upper part of (**a**) a picture of the transverse intensity profile of the forward beam is shown when the laser is attenuated by a filter. In this measurement the resolution is 0.01 nm

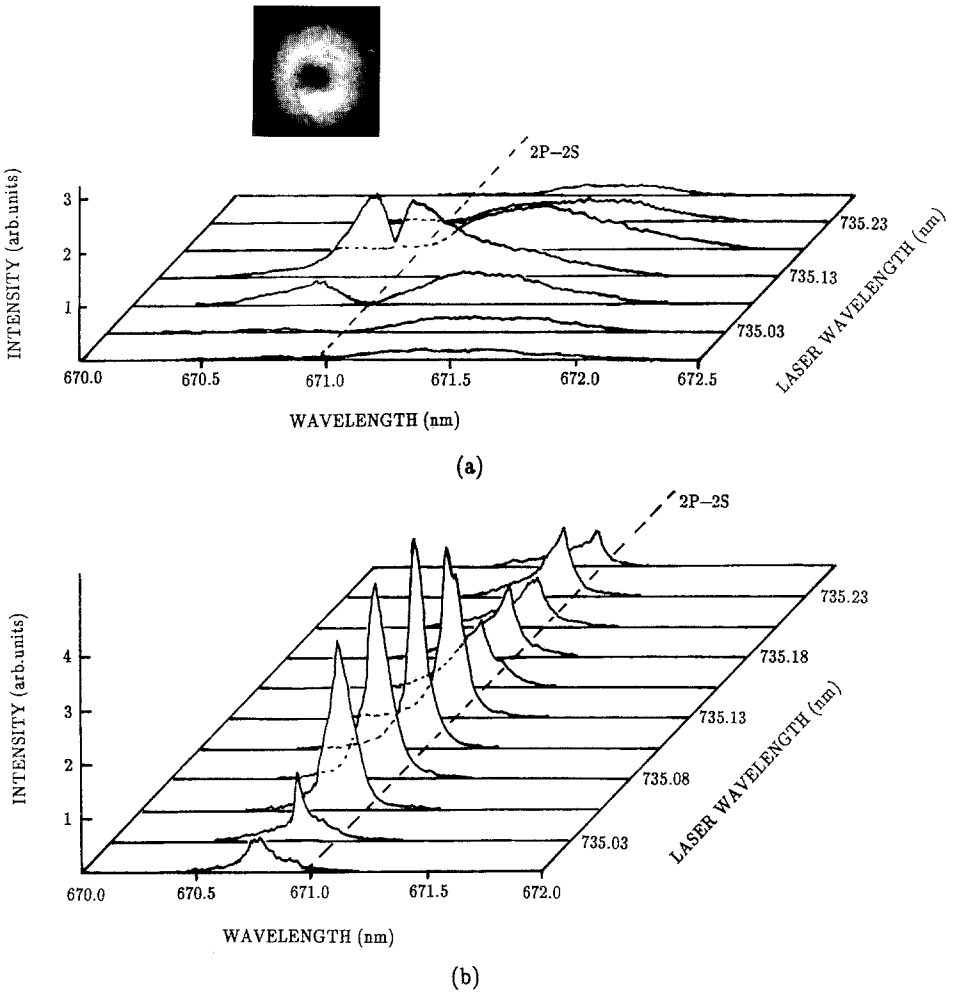

Fig. 5a, b. Spectra of the emissions near the 2P–2S transition, measured in the forward direction (**a**) and in the backward direction (**b**) as the laser is tuned near the 2S–3S two-photon resonance (735.13 nm). In the upper part of (**a**) a picture of the transverse intensity profile of the forward beam is shown when the laser is attenuated by a filter. In this measurement the resolution is 0.01 nm

has a broad band and changes the peak wavelength as the laser wavelength is tuned. Compared with Fig. 4b, where the measurement is made in the backward direction, this emission only appears in the forward direction. So it can be identified as PFWM due to phase-matching considerations. Actually, the complementary wave of this emission in the PFWM process can be found in the forward emission near the 2P–2S transition, which has the same broad band, as shown in Fig. 5a. Both the two emission beams have the shape of a cone surrounding the transmitted laser beam. The transverse intensity profiles of both emissions are shown in the upper parts of Figs. 4a and 5a, where the laser beam was strongly attenuated by a filter when the pictures were taken. The cone-shape means that this process is an angle phase-matched four-wave mixing. The bright spot at the center of the profile in Fig. 4a is due to the ASE corresponding to the 3S–2P transition and a small amount of laser emission which is left after filtering. However, in Fig. 5a there exists no light at the center of the profile due to the destructive interference that causes the ASE corresponding to the 2P–2S transition to disappear in the forward direction. From Figs. 4a, b, we find that the SHRS emission takes place only in the backward direction but not in the forward direction as the laser is detuned from the 2S–3S two-photon resonance. It indicates that the forward SHRS is completely suppressed.

In this case we evaluate the condition (1). First we calculate the 2S–3S two-photon Rabi frequency. Following Eicher's procedure [6] to calculate the dipole-matrix in (2), we have the 2S–3S two-photon Rabi frequency $\Omega_{2S-3S} = 197.28\, I_P$ rad/s, where I_P is in W/cm^2. Here, the laser intensity is about 2×10^8 W/cm^2 and the detuning Δ from the 2S–3S two-photon resonance is taken to be ~ 2 cm^{-1}, so (1) gives $R = 1.6 \times 10^{-3} \ll 1$, where the oscillator strength f_{ij} is taken from [6]. This R value indicates that the forward SHRS can not take place due to its negative gain. Notice that for the 3S–2P ASE a large signal can be clearly observed in the forward direction, see Fig. 4a, but only a very small signal can be found in close proximity of the resonance in the backward direction, see Fig. 4b. The reason is that the backward SHRS is so strong that the weak ASE can not be clearly observed in the same measurement. In order to reduce the influence of SHRS on the ASE measurement, the laser was detuned more than 0.2

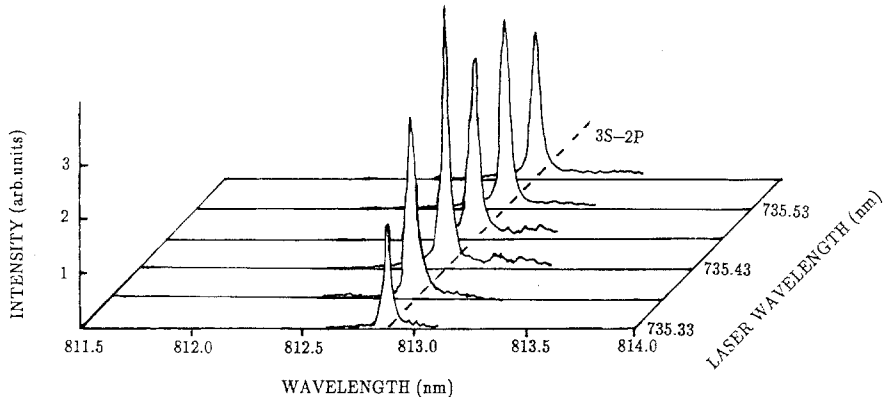

Fig. 6. Spectra of the emissions near the 3S–2P transition measured in the backward direction as the laser is detuned more than 0.2 nm to the long-wavelength side from the 2S–3S two-photon resonance. Here, the entrance slit of 30 μm and the exit slit of 30 μm are used. In this measurement the resolution is 0.03 nm

nm from the resonance to the long-wavelength side, which moves the SHRS signal far away from the ASE signal. Under this condition the backward ASE could be clearly observed with wider slits of the monochromator, and is shown in Fig. 6. Though the ASE signal is much weaker than the SHRS, it still has a good signal-to-noise ratio.

From Fig. 5b, two peaks can be seen in the spectrum of the backward emission as the laser is tuned on the 2S–3S two-photon resonance (735.13 nm). These two peaks should be considered due to the fine structure of the 2P state. As the laser is detuned to the short-wavelength side of the resonance, in the backward emission spectrum a remarkable shift of the peak frequency from the 2P–2S transition frequency ω_{2P-2S} can be found. By calculating, we find that these peak frequencies are exactly the same as those given by $2\omega_P - \omega_{3S-2P}$. For comparison the observed peak frequency and the calculated frequency with $2\omega_P - \omega_{3S-2P}$ are listed in Table 1. It means that the backward emission near the 2P–2S transition does not correspond to the 2P–2S transition. Actually, the process generating this emission is another new SHRS process induced by the 3S–2P ASE, as shown in Fig. 7. In the backward direction the 2P state is populated by the 2S–[3S]–2P SHRS process. In this new process the 2P state, as an initial state, absorbs a ω_{SHRS} photon generated by the 2S–[3S]–2P SHRS, emits both ω_{3S-2P} and ω' photons, and goes back to the ground state. This SHRS process, which we call an inverse SHRS just like inverse Raman scattering [7], has to be induced by the 3S–2P spontaneous emission of ω_{3S-2P} and is enhanced two-fold near resonance. Since the ω_{SHRS} photon only exists in the backward direction, this process can not be observed in the forward direction. In addition, no emission corresponding to the 2P–2S transition is found in the backward direction. This absence could be considered as a result of the competition between the 2P–2S transition and the 2P–[3S]–2S inverse SHRS process.

Table 1. Observed frequency and the frequency calculated with $2\omega_P - \omega_{3S-2P}$ for the backward emission near the 2P–2S transition as the laser is tuned to the short-wavelength side of the 2S–3S two-photon resonance

	Laser frequency ω_P [cm^{-1}]	ω' (observed) [cm^{-1}]	$2\omega_P - \omega_{3S-2P}$ [cm^{-1}]
2S–3S	13603.5	14904.9	14904.9
	13604.0	14905.7	14905.9
	13604.5	14906.6	14906.8
	13604.9	14907.7	14907.7
	13605.4	14908.8	14908.7

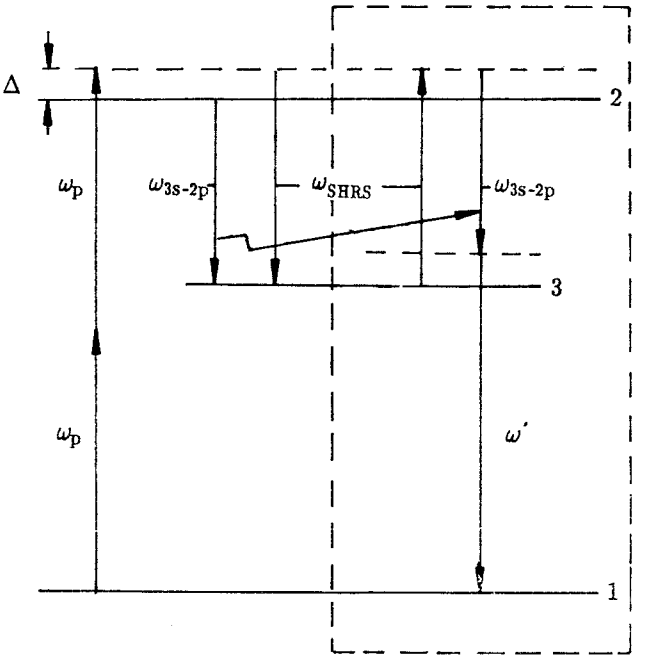

Fig. 7. Inverse SHRS process for generation of the emission corresponding to the $2\omega_P - \omega_{3S-2P}$ frequency (*right*, inside the block, framed with a *dashed line*). For comparison, the SHRS and ASE processes are also illustrated here (*left*).

The observed SHRS frequency value and its deviation from the $2\omega_P - \omega_{2P-2S}$ are listed in Table 2 in wavenumber, where the pump laser frequency is also included. It is found that the SHRS wavelength has a red shift from the calculated value as the laser is tuned to the long-wavelength side of the 2S–3S two-photon resonance. For

Table 2. Observed frequency and its deviation from the frequency calculated with $2\omega_P - \omega_{2P-2S}$ for the SHRS associated with the excitation of the 2P state as the laser is tuned near the 2S–3S or 2S–4S two-photon resonance. The corresponding laser frequency is also listed

	Laser frequency ω_P [cm^{-1}]	ω_{SHRS} (observed) [cm^{-1}]	$\omega_{SHRS} - (2\omega_P - \omega_{2P-2S})$ [cm^{-1}]
2S–3S	13598.4	12291.5	−1.4
	13599.4	12293.7	−1.1
	13600.3	12295.7	−0.9
	13601.2	12297.7	−0.8
	13602.1	12299.6	−0.6
	13603.1[a]	12301.7	−0.4
	13604.0	12303.7	−0.3
	13604.9	12305.5	−0.4
	13605.8	12307.3	−0.3
2S–4S	17504.8	20105.4	−0.2
	17505.4	20106.2	−0.6
	17506.0[b]	20107.8	−0.2
	17506.6	20109.2	−0.1
	17507.3	20110.2	−0.3
	17507.9	20111.5	−0.3
	17508.5	20112.9	−0.1
	17509.1	20114.1	−0.1
	17509.7	20115.5	0.1

[a] The resonant frequency for the 2S–3S two photon resonance.
[b] The resonant frequency for the 2S–4S two photon resonance.

small detuning the SHRS deviation of the observed value from the calculated value is within the uncertainty of this experiment, but for large detuning to the long-wavelength side the deviation becomes very large and is well resolved. Normally, these shifts might be considered being due to the Stark effect. Near the 2S–3S two-photon resonance the normal optical Stark effects of the 2S, 3S, $2P_{1/2}$, and $2P_{3/2}$ levels, given by (4), are $-0.3\ cm^{-1}$, $-0.04\ cm^{-1}$, $0.03\ cm^{-1}$, and $0.16\ cm^{-1}$, respectively. The Stark shift of the 2S or 3S level due to the two-photon Rabi frequency, given by (5), is $0.02\ cm^{-1}$ for $\Delta = -1.86\ cm^{-1}$ and $0.01\ cm^{-1}$ for $\Delta = -3.68\ cm^{-1}$. Actually, the observed deviation is $-1.1\ cm^{-1}$ at $\Delta = -7.4\ cm^{-1}$ and $-1.4\ cm^{-1}$ at $\Delta = -9.24\ cm^{-1}$, which are so large that it can not be explained by the Stark effects mentioned above.

When the laser is tuned near the 2S–4S two-photon resonance (571.23 nm), there exist two processes involved in the generation of SHRS (see Fig. 2). One is associated with the excitation of the 2P state and the other is associated with the excitation of the 3P state. For the SHRS associated with the 2P excitation the emissions near the 4S–2P transition and the 2P–2S transition were observed in both forward and backward directions as the laser wavelength scanned from 571.19 nm to 571.27 nm, and their spectra are shown in Figs. 8 and 9. In this case most of the results are similar to those observed near the 2S–3S two-photon resonance. Here, a cone-shaped beam in the forward direction was also observed, and the pictures of transverse intensity profile are shown in the upper parts of Figs. 8c and 9a. It indicates that an angle phase-matched PFWM process is also involved. However, from Fig. 8a only ASE signals can be seen. In order to observe the FWM signals, by using a 5 mm aperture only the central part of beam was measured and by using a 5 mm beam stop only the conic part of beam was measured. The results are shown in Fig. 8b, c. From Fig. 8c the PFWM signals can be clearly seen. From Fig. 8d, two different emissions were observed in the backward direction. One is from ASE and the other from SHRS, whose frequency is listed in Table 2, in which the deviation of the observed frequency from the calculated value and the laser frequency are included. All the deviations are well within the uncertainty of this experiment and no shift is found. In this case no SHRS was observed in the forward direction. Calculating (1) and (2), as we did above, for the 2S–4S two-photon Rabi frequency we have $\Omega_{2S-4S} = 28.77 I_P$ rad/s, where I_P is in W/cm^2. The laser intensity is $6 \times 10^8\ W/cm^2$, so $R = 3.7 \times 10^{-5}$. The condition $R \ll 1$ means that the forward SHRS is completely suppressed. The ASE related to the 2P–2S transition can be observed in the backward direction (see Fig. 9b) but not in the forward direction, which should be caused by the destructive interference between the two pathways connecting the 2S and 2P states. This interference only occurs in the forward direction. Contrary to the above 2S–3S case, here no inverse SHRS emission corresponding to the $2\omega_P - \omega_{4S-2P}$ was observed in the backward direction.

The same measurements were made for the SHRS associated with the 3P excitation. The results are shown in Figs. 10 and 11. A big difference is found between this case and the above two cases. In this case the ASE corresponding to the 4P–3S transition and the SHRS associated with the excitation of the 3P state could be observed in both the forward and backward directions. The frequencies of the pump laser and the SHRS observed in both directions are listed in Table 3, where the deviation of the observed value from the value calculated with $2\omega_P - \omega_{3P-2S}$ is included. From Table 3, a blue shift is found as the laser is tuned to the long-wavelength side from the 2S–4S two-photon resonance. By calculating (4), in this case the normal optical Stark shifts of 2S, 4S, $3P_{1/2}$, and $3P_{3/2}$ levels are $0.4\ cm^{-1}$, $0.15\ cm^{-1}$, $0.04\ cm^{-1}$, and $0.1\ cm^{-1}$, respectively. By calculating (5), the shift of the 2S or 4S level due to the two-photon Rabi frequency is 2×10^{-3}

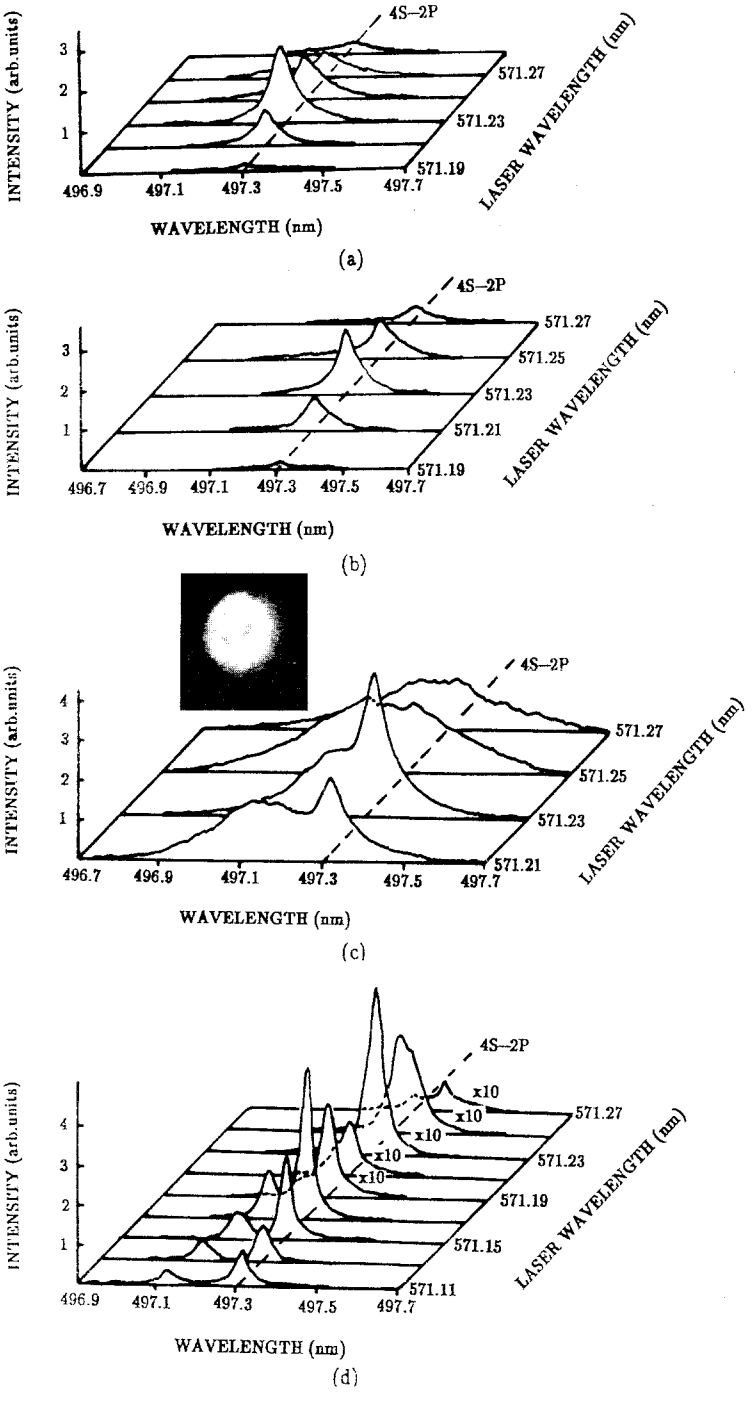

Fig. 8a–d. Spectra of the emissions near the 4S–2P transition measured in the forward direction without stop (**a**), with a 5 mm aperture stop (**b**), and with 5 mm beam stop (**c**), and in the backward direction (**d**) as the laser is tuned near the 2S–4S two-photon resonance (571.23 nm). In the upper part of (**c**) a picture of the transverse intensity profile of the forward beam is shown when the laser is eliminated by a filter. The resolution is 0.01 nm for (**a**) and (**b**), 0.02 nm for (**c**) and 0.03 nm for (**d**)

cm^{-1} for $\Delta = -3.68\ cm^{-1}$. However, the observed shift at $\Delta = -3.68\ cm^{-1}$ is about 1 cm^{-1}, which is so large that it can not be attributed to the Stark effect given above. We also notice that forward SHRS could be observed only when the laser is tuned to the long-wavelength side from the 2S–4S two-photon resonance, see Fig. 10a and Table 3. In this case, with similar calculations, we have $R = 0.12$, where $I_P = 6 \times 10^8\ W/cm^2$ and $\Delta = 2\ cm^{-1}$. If we consider that the transverse intensity profile of the laser beam has a Gaussian distribution and $R \propto I_P^2$, the much higher intensity of the central part of the beam could make the R to be larger than one. It means that the forward SHRS could take place. However, the forward SHRS is much weaker than the backward SHRS. The strong emission corresponding to the 3P–2S transition in the forward direction, see Fig. 11a, also indicates that the cancellation caused by the destructive interference between both pathways formed by the SHRS and FWM processes are not complete, and the real population in the 3P state exists.

In sodium under the experimental condition of [2], where the two-photon Rabi frequency $\Omega_{3S-4D} = 123 I_P$ rad s^{-1}, $\Delta = 1.2\ cm^{-1}$ and $I_P = 2 \times 10^7\ W/cm^2$, we have $R = 7.34 \times 10^{-3} \ll 1$. According to the condition (1), the forward SHRS should be completely suppressed, which agrees with the observation of [2].

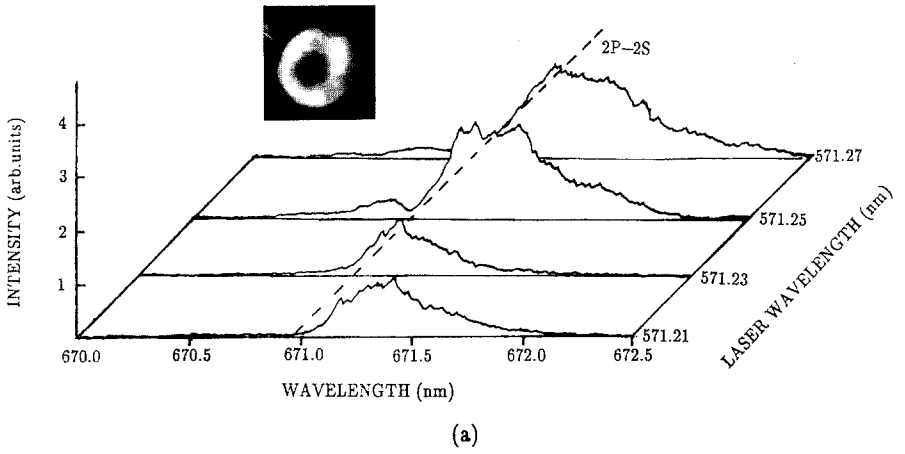

(a)

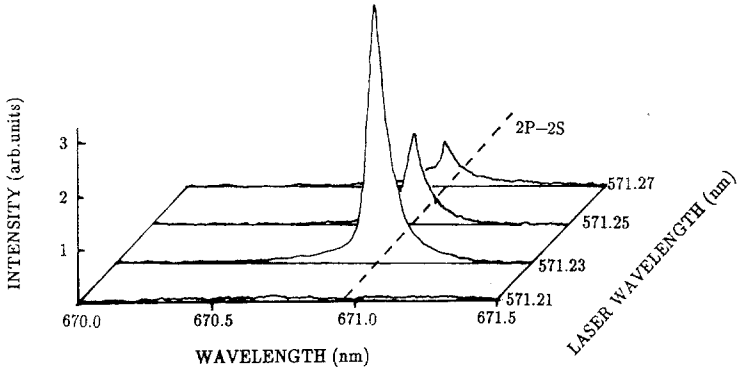

(b)

Fig. 9a, b. Spectra of the emissions near the 2P–2S transition measured in the forward direction (**a**) and in the backward direction (**b**) as the laser is tuned near the 2S–4S two-photon resonance (571.23 nm). In the upper part of (**a**) a picture of the transverse intensity profile of the forward beam is shown when the laser is eliminated by a filter. In this measurement the resolution is 0.02 nm

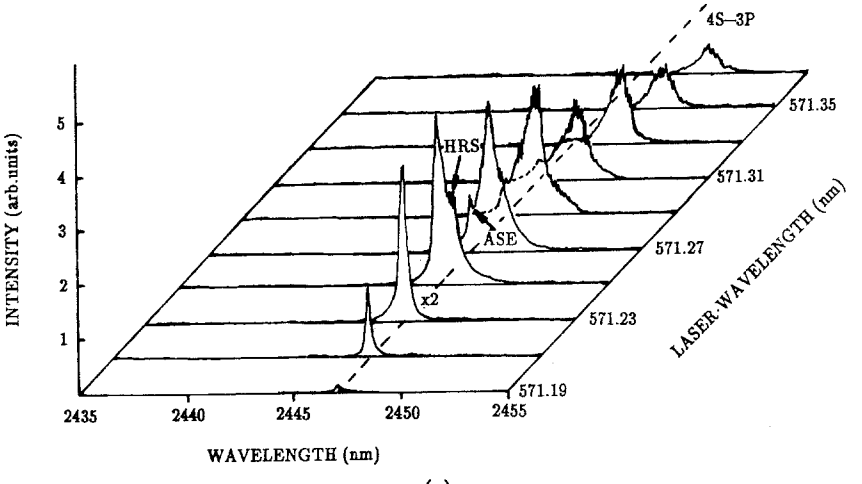

(a)

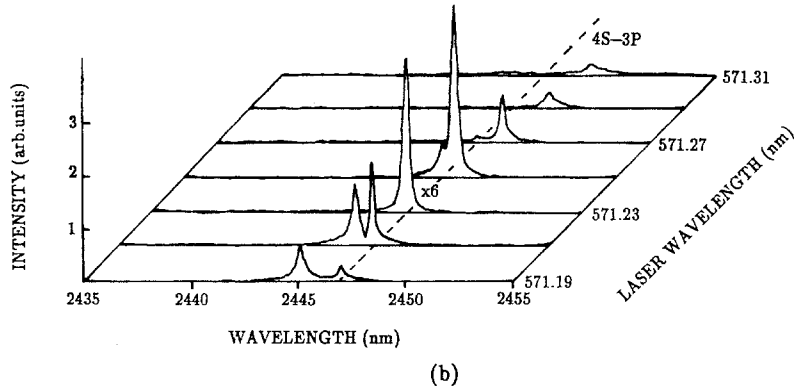

(b)

Fig. 10a, b. Spectra of the emissions near the 4S–3P transition measured in the forward direction (**a**) and in the backward direction (**b**) as the laser is tuned near the 2S–4S two-photon resonance (571.23 nm). The resolution is 0.12 nm for (**a**) and 0.06 nm for (**b**)

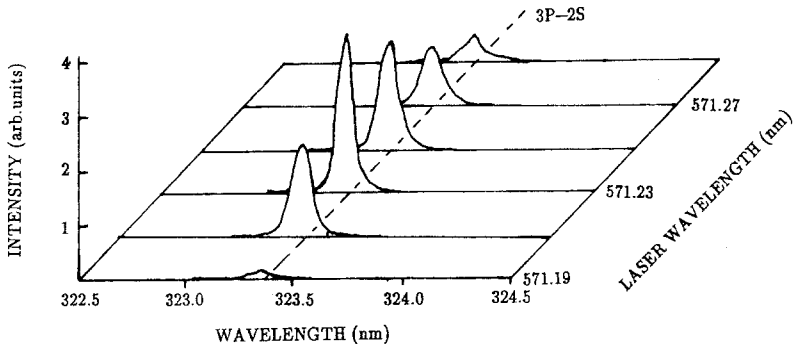

(a)

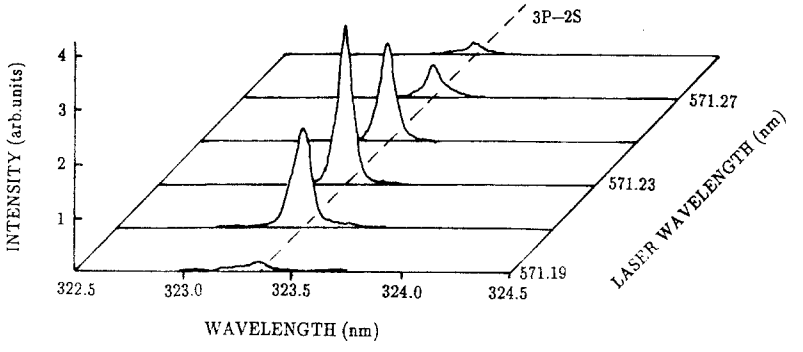

(b)

Fig. 11a, b. Spectra of the emissions near the 3P–2S transition measured in the forward direction (**a**) and in the backward direction (**b**) as the laser is tuned near the 2S–4S two-photon resonance (571.23 nm). In this measurement the resolution is 0.01 nm

Table 3. Frequency observed in both forward and backward directions and its deviation from the frequency calculated with $2\omega_P - \omega_{3P-2S}$ for the SHRS associated with the excitation of the 3P state as the laser is tuned near the 2S–4S two-photon resonance. The corresponding laser frequency is also listed

	Laser frequency ω_P [cm^{-1}]	ω_{SHRS} (observed) [cm^{-1}]		$\omega_{SHRS} - (2\omega_P - \omega_{3P-2S})$ [cm^{-1}]	
		Forward	Backward	Forward	Backward
2S–4S	17503.6	4083.1	4082.8	1.4	1.0
	17504.2	4084.1	4083.8	1.1	0.8
	17504.8	4084.6	4084.6	0.4	0.4
	17505.4	4085.5	4085.6	0.0	0.2
	17506.0[a]	4086.7	4086.6	0.0	0.0
	17506.6		4088.0	0.1	
	17507.3		4089.7	0.5	

[a] The resonant frequency for the 2S–4S two photon resonance

3 Conclusion

The SHRS in lithium was observed in both the forward and the backward directions as the laser was tuned near the 2S–3S and 2S–4S two-photon resonances. It is found that the forward SHRS emission associated with the excitation of the 2P state is completely suppressed, but the forward SHRS emission associated with the excitation of the 3P state can be observed. Under the condition of this experiment, condition (1) under which the forward SHRS takes place has been examined. For the SHRS associated with the 2P excitation, condition (1) gives $R \ll 1$. However, for the SHRS associated with the 3P excitation, condition (1) gives $R = 0.12$. If we consider the Gaussian distribution in the transverse intensity profile of laser beam and $R \propto I_P^2$, the fact that the forward SHRS associated with the 3P excitation takes place can be understood. All the results show that the predictions from (1) agree reasonably with the experimental results. We also examined condition (1) in the sodium case under the experimental condition of [2], a good agreement between the prediction and the observation is obtained.

Near the 2S–3S two-photon resonance, instead of the emission corresponding to the 2P–2S transition, an emission at the frequency $2\omega_P - \omega_{3S-2P}$, which is close to the frequency ω_{2P-2S}, has been observed in the backward direction. The process generating the emission of $(2\omega_P - \omega_{3S-2P})$ could be considered as an inverse SHRS induced

by the spontaneous emission of ω_{3S-2P}, and is illustrated in Fig. 7.

For the SHRS associated with the 2P excitation near the 2S–3S two-photon resonance a red shift has been observed. However, for the SHRS associated with the 3P excitation near the 2S–4S two-photon resonance a blue shift has been observed. In both cases the laser is tuned to the long-wavelength side of the resonance. In order to explain these shifts, the Stark effects have been calculated with (4) and under this experimental condition. Unfortunately, they are so small that the shifts of SHRS can not be attributed to them. The Stark effect induced by the backward SHRS is not considered because this effect should be much reduced for large detuning. The reason that causes the shift has not been understood yet.

Acknowledgement. This project was supported by National Science Council of R. O. C. under the grant No. NSC 80-0208-M009-41

References

1. M.A. Moore, W.R. Garrett, M.G. Payne: Opt. Commun. **68**, 310 (1988)
2. R.K. Wunderlich, W.R. Garrett, R.C. Hart, M.A. Moore, M.G. Payne: Phys. Rev. A **41**, 6345 (1990)
3. Y.P. Malakyan: Opt. Commun. **69**, 315 (1989)
4. S. Bashkin, J.O. Stoner, Jr.: *Atomic Energy Levels and Grotrian Diagrams*, Vol. 2 (North-Holland, Amsterdam 1975) p. 280
5. M.H. Lu, Y.M. Liu: Appl. Phys. B **54**, 288 (1992)
6. H. Eicher: IEEE J. **QE-*11*,** 121 (1975)
7. J. M. Hollas: *High Resolution Spectroscopy* (Butterworth, Washington 1982) p. 325